Dietary nitrite reverses features of postmenopausal metabolic syndrome induced by high-fat diet and ovariectomy in mice

Kazuo Ohtake[1] PhD, Nobuyuki Ehara[1] MS, Hiroshige Chiba[2] PhD, Genya Nakano[1] MS, Kunihiro Sonoda[3] MS, Junta Ito[4] PhD, Hiroyuki Uchida[1] PhD, and Jun Kobayashi[1] MD, PhD

[1]*Division of Pathophysiology, Department of Clinical Dietetics and Human Nutrition, Faculty of Pharmaceutical Science, Josai University, Saitama, Japan*
[2]*Laboratory of Applied Nutrition, Division of Pathophysiology Department of Nutrition and Life Science, Kanagawa Institute of Technology, Kanagawa, Japan*
[3]*Department of Food and Nutritional Environment, College of Human Life and Environment, Kinjo Gakuin University, Nagoya, Japan*
[4]*Division of Oral Anatomy, Department of Human Development and Fostering, Meikai University School of Dentistry, Saitama, Japan*

Authors' e-mail addresses
Kazuo Ohtake, PhD: kazuo@josai.ac.jp
Nobuyuki Ehara, MS: GVM1202@josai.ac.jp
Hiroshige Chiba, PhD: chiba@bio.kanagawa-it.ac.jp
Genya Nakano, MS: GVM1010@josai.ac.jp
Kunihiro Sonoda, MS: naka-k@kinjo-u.ac.jp
Junta Ito, PhD: junta.ito@dent.meikai.ac.jp
Hiroyuki Uchida, PhD: mrhiro@josai.ac.jp
Jun Kobayashi, MD, PhD: junkoba@josai.ac.jp

Corresponding author: Jun Kobayashi, MD, PhD,
Division of Pathophysiology, Department of Clinical Dietetics and Human Nutrition, Faculty of Pharmaceutical Science, Josai University, Saitama, Japan
E-mail address: junkoba@josai.ac.jp
Tel & Fax: +81-49-271-7223

Abstract
Menopausal women are at greater risk of developing metabolic syndrome with reduced endothelial nitric oxide synthase (eNOS) activity. Hormone replacement therapy increases eNOS activity and normalizes some characteristics of metabolic syndrome. We hypothesized that nitric oxide (NO) supplementation should have a therapeutic effect in this syndrome. We examined the effect of dietary nitrite on a mouse model with postmenopausal metabolic syndrome induced by ovariectomy (OVX) with a high-fat (HF) diet. C57BL/6 female mice were divided into five groups: sham+normal-fat (NF) diet, sham+HF, and OVX+HF without or with sodium nitrite (50 mg and 150 mg/L) in drinking water. Daily food intake and weekly body weight were monitored for 18 weeks. The OVX and HF groups showed significantly reduced plasma levels of nitrate/nitrite (NOx) and developed obesity with visceral hypertrophic adipocytes, and increased transcriptional levels of monocyte chemoattractant protein-1 (MCP-1), tumor necrotizing factor-α (TNF-α) and interleukin-6 (IL-6) in visceral fat tissues. The proinflammatory state in the adipocytes provoked severe hepatosteatosis and insulin resistance in the OVX+HF group compared with the sham+NF group. However, dietary nitrite significantly suppressed adipocyte hypertrophy and transcription of proinflammatory cytokine in visceral fat in a dose-dependent manner. The improvement of the visceral inflammatory state consequently reversed the hepatosteatosis and insulin resistance observed in the OVX+HF mice. These results suggest that an endogenous NO defect might underlie postmenopausal metabolic syndrome, and dietary nitrite provides an alternative source of NO, subsequently compensating for metabolic impairments associated with this syndrome.

Key words
nitrite
nitric oxide
postmenopause
metabolic syndrome
ovariectomy

Introduction

Recent studies show that nitric oxide (NO) deficiency might be a common underlying mechanism responsible for the development of metabolic syndrome (Monti LD 2003, Fernandez ML 2004, Cook S 2003, Huang PL 2009, Duplain H 2001), and that dietary nitrate and nitrite supplementations in animal models with this syndrome are effective in the treatment of dyslipidemia and insulin resistance (Jiang H 2014, Gilchrist M 2013, Stokes KY 2009). Carlström demonstrated that eNOS (endothelial nitric oxide synthase)-deficient mice treated with dietary nitrate had decreased visceral fat compared to untreated control mice, and that features of metabolic syndrome were reversed, suggesting that a central event in metabolic syndrome might be a decrease in NO bioavailability, and also that visceral hypertrophic adipocytes may be a potential target for actions of nitrate- and nitrite-derived NO (Carlström M, 2010).

On the other hand, the effect of NO supplementation on the development of metabolic syndrome in the postmenopausal state has not been studied. Menopausal women are at greater risk of developing metabolic syndrome in which estrogen deficiency predisposes them to cardiovascular diseases due to the increase in low-density lipoprotein cholesterol (Knopp RH 1994), and the decrease in vascular eNOS activity. This is likely due to reduced estrogen levels in menopause because hormone replacement therapy increases eNOS activity and normalizes some characteristics of metabolic syndrome (Cicinelli 1999, Majmudar NG 2000). Therefore, NO supplementation should have a therapeutic effect in this syndrome.

In the present study, we developed ovariectomized (OVX) mice fed with a high-fat (HF) diet, then characterized inflammatory and metabolic profiles of this model and also investigated the therapeutic effects of dietary nitrite supplementation on the development of the experimental postmenopausal metabolic syndrome model of mice.

Materials and Methods

Experimental procedures

Specific pathogen-free female C57BL/6J mice, 10 week of age from CLEA Japan, Inc. (Tokyo, Japan) were allowed food (CE-2, CLEA Japan) and reverse osmosis (RO) water ad libitum, and were kept on a 12/12 h light/dark cycle with at least 7 days of local vivarium acclimatization before experimental use. All the protocols were approved by the Institutional Animal Care and Use Committee at the University of Josai Life Science Center (H23014) and were consistent with the Guide for the Care and Use of Laboratory Animals published by the NIH. In order to examine if mice with or without ovariectomy were fed either a normal-fat (NF, 10%) or high-fat (HF, 60% fat from lard) diet (Table 1), at 11 wk of age, animals were anesthetized with intraperitoneal injection of pentobarbital (60 mg/kg) under aseptic conditions and underwent ovariectomy (OVX) or sham surgery. Vaginal smears were examined for cytology twice during the experiment (2 and 18 weeks after OVX) to confirm that all mice were being killed at the same stage of the estrous cycle (Ludgero-Correia A 2012). After a one week resting period, mice were matched for body composition (n = 8 per group) and rerandomized into five groups: 1) Sham mice fed with NF diet (sham+NF), 2) Sham mice fed with HF diet (sham+HF), 3) OVX mice fed with HF diet (OVX+HF), 4) OVX mice fed with HF diet and 50 mg/L nitrite in drinking water (OVX+HF+N50), and 5) OVX mice fed with HF diet and 150 mg/L nitrite in drinking water (OVX+HF+N150). Both NF and HF diets were produced by Oriental Yeast Co. Ltd. (Tokyo, Japan), in accordance with AIN-93M recommendations (Reeves 1993). The diets' compositions are detailed in Table 1.

The mice were housed in individual cages in a temperature and humidity controlled room. Obesity was confirmed by checking body weight (once a week) for 18-week experimental period (Ludgero-Correia 2012). At 30 weeks of age, the animals were anesthetized with an intraperitoneal injection of pentobarbital (60 mg/kg) following a 16 hour fasting period. To determine the homeostasis model assessment as an index of insulin resistance (HOMA-IR), blood samples (about

0.5 ml) were collected from the abdominal aorta and transferred into plastic tubes containing sodium EDTA. Blood glucose levels were determined with Glucocard™ (GT-1661, Arkray, Inc., Kyoto, Japan). Plasma insulin concentrations were determined with Mouse Insulin ELISA kit (Shibayagi, Gunma, Japan). HOMA-IR was calculated as fasting plasma glucose [mmol/l] × fasting plasma insulin [mU/l] / 22.5 (Liu 2010). Thereafter, visceral adipose tissues (ovarian fat mass) and liver were then excised from animals and frozen immediately at -80°C until use or fixed in 10% (w/v) neutral buffered formalin solution. Uterine mass was also measured after euthanasia to ensure the success of the ovariectomy.

RT-PCR

Tissue samples (adipose and liver) stored at −80°C were extracted using RNeasy Lipid Tissue Mini kit (QIAGEN) according to the manufacturer's instructions. Total RNA concentrations were quantified by NanoDrop system (Thermo Fisher Scientific™). RT-PCR was performed with 1 μg of total RNA by use of Gene RED PCR Mix (NIPPON GENE) according to the manufacturer's instructions: 1 cycle at 42°C for 40 min, 95°C for 5 min, and 4°C for 5 min for reverse transcription; and 23-36 cycles at 94°C for 30 s, 60°C for 30 s, and 72°C for 1 min for PCR. PCR was performed with a RoboCycler 96 gradient temperature cycler (Stratagene). The oligonucleotides used as primers were synthesized by FASMAC (Kanagawa, Japan). The primer pairs were designed as follows, glyceraldehyde-3-phosphate dehydrogenase (GAPDH): forward primer, 5′-agaacatcatccctgcatcc′,reverse primer, 5′-tccaccaccctgttgctgta-3′ (367 bp, 25 cycle), TNF-α: forward primer, 5′-ggcaggtctactttggagtcattgc-3′, reverse primer, 5′-acattcgaggctccagtgaattcgg-3′ (300 bp, 35 cycle), MCP-1: forward primer, 5′-actgaagccagctctctcttcctc′, reverse primer, 5′-ttccttcttggggtcagcacagac-3′ (274 bp, 31 cycle), IL-6: forward primer, 5′-acttccatccagttgccttct-3′, reverse primer, 5′-gaattgccattgcacaactct-3′ (199 bp, 36 cycle), Adiponectin: forward primer, 5′-gggtgagacaggagatgttggaatg-3′, reverse primer, 5′-gccagtaaatgtagagtcgttgacg-3′ (478 bp, 23 cycle), β_3-Adrenergic Receptor: forward primer, 5′-tgcgcccatcatgagccagtggtg-3′, reverse primer, 5′-gcgaaagtccgggctgcggcagta-3′ (300 bp, 27 cycle), uncoupling protein-1 (UCP-1): forward primer, 5′-gggcccttgtaaacaacaa-3′, reverse primer, 5′-gaagccacaaacccttttga-3′ (223 bp, 32 cycle), peroxisome proliferator-activated receptor-γ (PPAR-γ): forward primer, 5′-cgtgatggaagaccactcgc-3′, reverse primer, 5′-aacctgatggcattgtgaga-3′ (477 bp, 27 cycle), CCAAT/enhancer-binding protein-α (C/EBP-α): forward primer, 5′-cggtggacaagaacagcaac-3′, reverse primer, 5′-cggaatctcctagtcctggc-3′ (365 bp, 33 cycle), sterol regulatory element binding protein-1c (SREBP-1c): forward primer, 5′-tgcacacaaaagcaaatcactgaag-3′, reverse primer, 5′-attagagccatctctgctctc-3′ (436 bp, 33 cycle), acetyl-CoA carboxylase (ACC): forward primer, 5′-aatgcatgcgatctatccgtc-3′, reverse primer, 5′-tcttgccaatccactcgaaga-3′ (418 bp, 30 cycle), acyl CoA oxidase (ACO): forward primer, 5′-cttgttcgcgcaagtgagg-3′, reverse primer, 5′-caggatccgactgtttacc-3′ (213 bp, 25 cycle), middle-chain acyl-CoA dehydrogenase (MCAD): forward primer, 5′- tggagacattgccaatcagc-3′, reverse primer, 5′- accatagagctgaagacagg-3′ (355 bp, 25 cycle), G6Pase: forward primer, 5′-aggcatgcagagtctttggt-3′, reverse primer, 5′-accgcaagagcattctcagt-3′ (302 bp, 25 cycle), phosphoenolpyruvate carboxykinase (PEPCK): forward primer, 5′- tctatgaagccctcagctgg-3′, reverse primer, 5′- tctgtgctactcaactgact -3′ (691 bp, 25 cycle). Target mRNA expressions were quantified relative to the expression of GAPDH. A portion of each PCR mixture was electrophoresed in 2% agarose gel in TBE buffer (89 mM Tris, 89 mM boric acid, 2 mM EDTA, pH 8.3), and the gel was visualized by ethidium bromide staining. The intensity of the PCR products was measured using a Gene Genius Bioimaging System (Syngene).

Histological analysis

Adipose tissues and liver were fixed in 10% neutral buffered formalin solution and embedded in paraffin. Sections (8 μm) were stained with hematoxylin and eosin (HE) for light microscopic observation at ×200 magnification. The mean area of adipocyte in ovarian fat was calculated by measuring the area of 500 individual adipocytes per 20 randomly chosen fields per ovarian fat section in each experimental group (n=8/group) using the Image J software program (Okuno 1998). The ratio of the fat area to the total area of the specimen cross-section of liver was determined by measuring the microscopic area of fat vacuole and the total area of vision from 10 different fields per liver section in each experimental group (n=8/group) using the Image J software program (Lim 2013). Digital images were obtained from a high-resolution digital camera system (Penguin 150CL, Pixera, Los Gatos, CA, USA) linked to a microscope (BX41, Olympus, Tokyo, Japan) and desktop computer (Pentium 4, 2.0 GHz).

Nitrite and nitrate concentrations in the plasma

Nitrite and nitrate concentrations in the plasma were measured using a dedicated HPLC system (ENO-20; EiCom, Kyoto, Japan) (Ohtake 2007, Ohtake 2010). This method is based on the separation of nitrite and nitrate by ion chromatography, followed by on-line reduction of nitrate to nitrite, postcolumn derivatization with Griess reagent, and detection at 540 nm. Proteins in each sample were removed by centrifugation at 10,000*g* for 5 min following methanol precipitation (plasma:methanol = 1:1 volume /volume, 4 °C).

Statistical analysis

All values are expressed as means ± SE. Data were analyzed by one or two-way ANOVA, and then differences among means were analyzed using the Tukey-Kramer multiple comparison test. A level of $P < 0.05$ was considered significant.

Results

Surgery-induced menopause

To confirm successful surgically induced menopause in this mouse model, vaginal cytology and uterine mass were analyzed. The vaginal smears showed the predominance of leukocytes characteristic of the diestro stage of the rodent's estrous cycle. Because uterine weight of OVX female mice is well correlated with the plasma levels of estradiol (Wang Y 2015), uterine weight is often used as a surrogate measure of biologically active estrogen (Elliot SJ et al. 2003). Uterine mass of OVX groups was significantly decreased compared to that of the sham groups irrespective of whether or not the mice were fed an HF diet and dietary nitrite, indicating that uterus atrophy and postmenopausal status are successfully induced by OVX (Fig. 1A).

Effect of dietary fat and nitrite on body mass

Figure 1B shows the time course of body mass change in the sham and OVX mice treated with or without an HF diet and dietrary nitrite. The sham+HF group showed a higher body mass than the sham+NF group, with significant differences ($p<0.05$) from 4 weeks to 18 weeks. The OVX+HF groups (both with and without nitrite) showed a higher body mass than the sham groups (both NF and HF), with significant differences ($p<0.05$) from 1 week to 18 weeks. Regardless of whether or not the mice were fed dietary nitrite, there was no difference among the OVX+HF groups, suggesting that dietary nitrite had no impact on body mass in the OVX+HF groups.

Effect of HF diet and dietary nitrite on morphometry of visceral adipocytes

Figure 2A shows the ratio of ovarian fat mass to whole body mass in the 5 groups. The HF diet increased this ratio in the sham+HF and OVX+HF groups compared to the sham+NF group. On the

other hand, nitrite supplementation in the OVX+HF group dose-dependently decreased this ratio. In the microscopic examination, among the 5 groups, the HF diet increased the size of ovarian adipocytes, which were more augmented with the addition of OVX (Fig. 2B). Crown-like structures indicative of a necrotic adipocyte surrounded by macrophages are frequently observed in OVX+HF groups (arrow in Fig. 2C) (Murano I, 2008). Consistent with the changes of ratio of ovarian fat mass to whole body mass (Fig. 2A), nitrite supplementation in the OVX+HF group significantly decreased the size of adipocytes (Fig. 2B and 2C).

Transcriptional levels of cytokines in ovarian adipose tissue

Based on the evidence that the visceral hypertrophic adipocytes play a causative role in the development of metabolic syndrome by releasing inflammatory cytokines to the portal and systemic circulation (Franklin RM, 2009), we measured the transcriptional levels of inflammatory cytokines (TNF-α, IL-6, and MCP-1) (Fig. 3A) and adipocyte-related biomarkers (adiponectin, β2-adrenagic receptor, UCP-1, PPAR-γ and C/EBP-α) (Fig. 3B) in ovarian fat tissue. The mRNA levels of TNF-α, IL-6, and MCP-1 increased in the HF diet group compared to the sham+NF, and higher increases were observed in the OVX+HF group than in the sham groups (sham+NF and sham+HF), whereas these were significantly suppressed by dietary nitrite (in OVX+HF+N50, and +N150) (Fig. 3A). On the other hand, there was no significant difference in mRNA levels of adiponectin, energy consumption-related (β2-adrenagic receptor and UCP-1) and adipocyte differentiation-related factors (PPAR-γ and C/EBP-α) among the 5 groups (Fig. 3B).

Effect of dietary nitrite on OVX and HF diet-induced fatty liver

Because portal delivery of proinflammatory cytokines and FFAs from visceral adipocytes induces fatty liver in obesity-induced metabolic syndrome (Shoelson SE, 2006), we examined liver histomorphology. As shown in Figure 4A, there were many more lipid droplets in the hepatocytes of the sham+HF group than the sham+NF group, and the most lipid droplets were observed in the OVX+HF group, whereas dietary nitrite apparently reduced the number of lipid droplets in the hepatocytes of the OVX+HF+N50 and +N150 groups in a dose-dependent manner. The suppressive effect of dietary nitrite on OVX and HF diet-induced fatty liver is also qualitatively presented in Figure 4B (the ratio of the total fat vacuole area). We also measured hepatic mRNA levels of the regulating factors closely related to hepatic lipid metabolism, such as SREBP-1c and ACC for lipogenesis, ACO and MCAD for fatty acid β-oxidation, G6Pase and PAPCK for glycogenesis (Fig. 5). OVX and HF diet significantly increased SREBP-1c, and this was dose-dependently reversed by the addition of dietary nitrite. This was also observed in ACC transcription but was not significant. This suggests that at least lipogenesis due to enhanced SREBP-1c expression might be one of the contributors to the development of fatty liver in this model. However, OVX, HF diet and dietary nitrite had no impact on the other hepatic transcriptional levels in this model (Fig. 5).

Effect of dietary nitrite on glucose metabolism and insulin sensitivity

Figure 6 shows significant increases in the levels of fasting blood glucose (Fig. 6A) and plasma insulin (Fig. 6B) in the OVX+HF group compared to the sham+NF group. Although dietary nitrite did not affect blood glucose levels, plasma insulin levels decreased dose-dependently with dietary nitrite. To assess fasting insulin sensitivity, HOMA-IR was calculated, which exhibited an increased insulin resistance in the OVX+HF group, and dietary nitrite dose-dependently improved insulin sensitivity (Fig. 6C).

Plasma levels of nitrate/nitrite

We measured plasma levels of nitrate/nitrite (NOx) as a measure for endogenous NO production in fasting (Fig. 7). Plasma NOx levels significantly decreased in the OVX+HF group compared to the sham groups. Although the difference did not reach statistical significance, plasma NOx levels

tended to increase with nitrite supplementation, possibly reflecting the compensation for the lack of NO in the OVX+HF mice.

Discussion

The present study showed that dietary nitrite improved several features observed in the OVX+HF mice model of postmenopausal metabolic syndrome. It is well-accepted that dietary nitrate and nitrite act as a substrate for systemic NO generation, serving as a physiological alternative source of NO-based signaling when endogenous NOS-derived NO is lacking (Bryan NS 2005). Recent accumulating evidence has suggested that polymorphism in the eNOS gene is associated with the development of metabolic syndrome in humans (Fernandez ML 2004, Monti LD 2003), and eNOS-deficient mice display a number of features of metabolic syndrome, such as hypertension, dyslipidemia, and insulin resistance (Gonzalez-Sánchez 2007), thereby indicating that loss of NO bioavailability might be an important underlying molecular mechanism for the development of metabolic syndrome (Carlström 2010). Consistent with these reports, the present study also showed a significant decrease in plasma NOx levels in OVX+HF postmenopausal metabolic mice compared to sham+NF control mice. Although statistical significance of plasma NOx levels could not be observed in the OVX+HF group between cases with and without dietary nitrite, there was an apparent tendency for increased plasma NOx levels following nitrite supplementation (Fig. 7), which accordingly improved the metabolic and histological features of the experimental postmenopausal syndrome. NO plays suppressive roles in the development of metabolic syndrome at various levels of this process, including regulation of microvascular blood flow (Wang 2013), mitochondrial function (Larsen 2011), insulin secretion (Nystrom 2012), glucose uptake (Khoo 2014), and modulation of inflammation (Rizzo 2010). In the present study, we believe the inhibition of visceral proinflammatory cytokine expression with dietary nitrite might be the central event in the subsequent curing process of this syndrome. Recent studies suggest that long-chain saturated FFAs derived from excess adiposity induce inflammatory mediators by toll-like receptor-4 (TLR4)-mediated NF-κβ activation (de Luca 2008, Dasu 2011), and inactivation of NF-κβ by nitrosative modification of IκκB could suppress TLR4-mediated signal propagation of the proinflammatory cytokines (Hess DT 2005). Although further investigations will be required to answer this in more detail, focusing on a more definite signaling mechanism of phosphorylation and nitrosation for this process, the present study showed that dietary nitrite suppressed the inflammatory cytokine transcription in the visceral adipocytes, possibly inhibiting subsequent systemic inflammatory responses, including hepatic steatosis and insulin resistance in skeletal muscles (Shoelson 2006 ,Yuan M 2001).

On the other hand, the effect of NO supplementation on metabolic syndrome in the postmenopausal state has not been well studied so far. In this study, although we did not measure plasma estrogen levels, uterine mass, which is often used as a surrogate measure of biologically active estrogen (Wang Y 2015), was significantly decreased in the OVX groups compared to the sham groups, indicating that uterus atrophy mimics the postmenopausal state. The effect of gender differences in the prevalence of cardiovascular disease and its increasing risk in postmenopausal women are well-known (Cicinelli 1999). Furthermore, recent reports suggested that menopause in women reduces eNOS activity and estrogen replacement therapy increases the plasma NOx levels and improves endothelium-dependent vascular functions through estrogen receptor-mediated activation of eNOS (Cicinelli E 1999, Chen Z 1999). As reported in a previous study (Ludgero-Correia 2012), here we showed the apparently accelerating development of metabolic syndrome in the menopausal state with the additional treatment of OVX mice with an HF diet, and this was consequently improved by dietary nitrite in a dose-dependent manner. These results suggest that dietary nitrite supplementation in postmenopausal metabolic syndrome might restore NO bioavailability and compensate for the metabolic consequences of estrogen deficiency.

Next, we investigated the detailed effects of dietary nitrite on fat and glucose metabolism in this model. Either OVX+HF diet or dietary nitrite had little impact on the hepatic transcriptional level of ACC (a regulating factor for lipogenesis), whereas SREBP-1c, another major transcriptional regulator for lipogenic genes increased with the HF diet and increased even more with additional OVX treatment, resulting in hepatosteatosis in an OVX+HF group (Murase 2001). Endo et al. reported that TNF-α induces hepatosteatosis in mice by enhancing gene expression of SREBP-1c (Endo 2007); therefore, increased hepatic lipogenesis by SREBP-1c is likely to be suppressed by dietary nitrite via reduction of proinflammatory cytokines in visceral and hepatic adipocytes. On the other hand, among all 5 groups there was no change in hepatic transcriptional levels of ACO, MCAD, G6Pase and PAPCK, suggesting that, rather than fatty acid β oxidation and glycogenesis, lipogenic regulation might be responsible for the development of fatty liver in this postmenopausal mouse model. In contrast to the present result, previous reports demonstrated a causative relation of G6Pase to hepatosteatosis (Konopelska 2011). However, because lipid metabolism in the liver is highly nutritionally and hormonally regulated at the transcriptional level (Yamamoto 2004), and is often reported discrepantly (Gregoire 2002, Kim 2004), further studies will be needed to clarify this complicated and multifactorially balanced lipid homeostasis in particular focusing on different conditions, such as fed, fasted, and refed, as well as gender, ageing and menopause.

Next we examined alterations of glucose homeostasis following the treatments of OVX and/or HF diet and also examined the therapeutic effect of dietary nitrite on the impaired glucose tolerance. Significant increases in fasting plasma levels of glucose and insulin were observed in the OVX+HF group compared to the sham+NF group, and these were dose-dependently reversed with dietary nitrite (Fig. 6A, B). HOMA-IR also revealed an increased insulin resistance in the OVX+HF group and this was also improved with dietary nitrite (Fig. C). Based on the previous evidence that insulin-related signal transduction is impaired by enhanced inflammatory cytokines and reactive oxygen species (Guiherme 2008), here we try to discuss the effect of dietary nitrite on the insulin signaling process in OVX+HF mice. Elevated FFAs inhibit insulin signaling through the activation of TLR4-mediated NF-κβ and NADPH oxidase, which are followed by the stimulation of inflammatory mediators (TNF-a, IL1B, IL-6, and PKC) and serine phosphorylation of insulin receptor substrate-1 (IRS-1), thereby leading to insulin resistance (Guiherme 2008). As mentioned above, it might be possible that dietary nitrite-mediated nitrosative modification and inhibition of IκκB/NF-κβ signaling axis are the start of the reversal in glucose homeostasis and insulin resistance[LSC1] (Hess 2005). In addition, Jiang recently reported that dietary nitrite improves insulin resistance through a glucose transporter 4 (GLUT4)-mediated mechanism, in which NO-dependent nitrosation of GLUT4 facilitates GLUT4 translocation to the membrane for glucose uptake and thereby improves insulin resistance (Jiang 2014). Further work is still needed. Nitrosative modification of the signal-related proteins could be involved in the impaired glucose tolerance underlying postmenopausal metabolic syndrome.[LSC2]

When considering an application of this treatment to clinical practice, there are a couple of issues to be considered. First, there is the question of how dietary nitrite exerts NO activity in vivo. In general, while most dietary nitrate and nitrite (mostly from fruit, vegetables, and water[LSC3]), including oxidation products of endogenous NO, is excreted into the urine, 25% of dietary nitrate is recycled to saliva through the enterosalivary pathway, followed by bacterial reduction to nitrite in the oral cavity, is then acid-catalyzed in the stomach for the formation of NO and *S*-nitrosated proteins (*S*-nitrosoglutathione, *S*-nitrosocysteine). Although NO, a short-lived gaseous molecule, plays an important role in local defense in the gastric mucosa, *S*-nitrosated proteins and nitrite, which are more stable NO donors, are absorbed in the upper gastrointestinal tract and are delivered systemically, subsequently serving as transnitrosation agents and/or on-demand NO donors. We

applied dietary nitrite instead of dietary nitrate, because rodents such as rats and mice do not actively concentrate circulating nitrate in saliva (enterosalivary route) (Djekoun-Bensoltane G 2007, Cockburn A 2013, Montenegro MF 2016). Therefore, the present study was thus designed to simulate the human-like enterosalivary cycle by applying dietary nitrite.

The second issue is whether the dose of dietary nitrite is consistent with that of human diets. The amounts of nitrite used in the present study totaled approximately 0.1 and 0.3 mg/day for mice drinking the lower and higher doses of nitrite, respectively (based on drinking 2 ml of water per day) and these increased steady-state plasma NOx levels. These doses of nitrite are orally achievable through increasing consumption of nitrate/nitrite-rich foods and vegetables (Bryan 2007), providing a possible therapeutic strategy for patients with postmenopausal metabolic syndrome.

Another issue to discuss is safety of the dose of dietary nitrite used in this mice model. It was reported that elevated nitrate doses in well water were associated with infantile methemoglobinemia and low blood pressure (Comly HH 1945, Knobeloch L 2000). However, because no gross fetal pathology was observed in the present mice model, we did not measure methemoglobin levels and blood pressure. We previously reported a mouse model for experimental colitis treated with 25 mmol/L sodium nitrite in drinking water (approximately 35- and 12-fold concentrated nitrite levels compared to those of the present study); however, even at that dose, no measurable effects on methemoglobin levels and blood pressure were observed (Ohtake 2010).

Regarding the relation of dietary nitrate and nitrite to nitrosamine formation and cancer development, although it is outside the scope for this research work, so far there has been no evidence supporting the role of fruit and vegetables in cancer development. Although more detailed reviews are available (Bradbury KE 2014), dietary nitrate and nitrite, at least from plant-based foods, have obviously inhibitory effects on cancer and even cardiovascular risk by playing some synergistic role with other nutrients, such as vitamins C and E, and polyphenols in these foods, rather than forming *N*-nitroso-compounds including nitrosamine (Kobayashi J 2015).

In conclusion, these results suggest that an endogenous NO defect might underlie postmenopausal metabolic syndrome; therefore, dietary nitrite provides an alternative source of NO, and subsequently compensates for metabolic impairments associated with this syndrome.

References

Bradbury KE, Appleby PN, Key TJ. Fruit, vegetable and fiber intake in relation to cancer risk; findings from the European Prospective Investigation in to Cancer and Nutrition (EPIC). *Am J Clin Nutr* 100: 394S-398S, 2014.

Bryan NS, Fernandez BO, Bauer SM, Garcia-Saura MF, Milsom AB, Rassaf T, Maloney RE, Bharti A, Rodriguez J, Feelisch M. Nitrite is a signaling molecule and regulator of gene expression in mammalian tissues. *Nat Chem Biol* 1: 290-297, 2005.

Bryan NS, Calvert JW, Elrod JW, Gundewar S, Ji SY, Lefer DJ. Dietary nitrite supplementation protects against myocardial ischemis-reperfusion injury. *Proc Natl Acad Sci* 104: 19144-19149, 2007.

Carlström M, Larsen FJ, Nyström T, Hezel M, Borniquel S, Weitzberg E, Lundberg JO. Dietary inorganic nitrate reverses features of metabolic syndrome in endothelial nitric oxide synthase-deficient mice. *Proc Natl Acad Sci* 107: 17716–17720, 2010.

Chen Z, Yuhanna IS, Galcheva-Gargova Z, Karas RH, Mendelsohn ME Shaul PW. Estrogen receptor α mediates the nongenomic activation of endothelial nitric oxide synthase by estrogen. *J*

Clin Invest 103: 401-406, 1999.

Cicinelli E, Ignarro LJ, Matteo MG, Galantino P, Schonauer LM, Falco N. Effects of estrogen replacement therapy on plasma levels of nitric oxide in postmenopausal women. *Am J Obstet Gynecol* 180: 334-339, 1999.

Comly HH. Cyanosis in infants caused by nitrates in well water. *JAMA* 129: 112-116, 1945.

Cook S, Hugli O, Egli M, Vollenweider P, Burcelin R, Nicod P, Thorens B, Scherrer U. Clustering of cardiovascular risk factors mimicking the human metabolic syndrome X in eNOS null mice. *Swiss Med Wkly* 133: 360-363, 2003.

Dasu MR, Jialal I. Free fatty acids in the presence of high glucose amplify monocyte inflammation via Toll-like receptors. *Am J Physiol Endocrinol Metab* 300: E145-E154, 2011.

de Luca C, Olefsky JM. Inflammation and insulin resistance. *FEBS let* 582: 97-105, 2008.

Duplain H, Burcelin R, Sartori C, Cook S, Egli M, Lepori M, Vollenweider P, Pedrazzini T, Nicod P, Thorens B, Scherrer U. Insulin resistance, hyperlipidemia, and hypertension in mice lacking endothelial nitric oxide synthase. *Circulation* 104: 342-345, 2001.

Elliot SJ, Kari M, Berho M, Potier M, Zheng F, Leclercq B, Striker GE, Striker LJ. Estrogen deficiency accelerates progression of glomerulosclerosis in susceptible mice. *Am J Pathol* 162: 1441-1448, 2003.

Endo M, Masaki T, Seike M, Yoshimatsu H. TNF-alpha induces hepatic steatosis in mice by enhancing gene expression of sterol regulatory element binding protein-1c(SREBP-1c). *Exp Biol Med* 232: 614-621, 2007.

Fernandez ML, Ruiz R, Gonzalez MA, Ramirez-Lorca R, Couto C, Ramos A, Gutierrez-Tous R, Rivera JM, Ruiz A, Real LM, Grilo A. Association of NOS3 gene with metabolic syndrome in hypertensive patients. *Thromb Haemost* 92: 413-418, 2004.

Franklin RM, Ploutz-Snyder L, Kanaley JA. Longitudinal changes in abdominal fat distribution with menopause. *Metabolism* 58: 311-315, 2009.

Gilchrist M, Winyard PG, Aizawa K, Anning C, Shore A, Benjamin N. Effect of dietary nitrate on blood pressure, endothelial function, and insulin sensitivity in type 2 diabetes. *Free Rad Biol Med* 60: 89-97, 2013.

Gonzalez-Sánchez JL, Martinez-Larrad MT, Saez ME, Zabena C, Martinez-Calatrava MJ, Serrano-Rios M. Endothelial nitric oxide synthase haplotypes are associated with features of metabolic syndrome. *Clin Chem* 53: 91-97, 2007.

GregoireFM, Zhang Q, Smith SJ, Tong C, Ross D, Lopez H, West DB. Diet-induced obesity and hepatic gene expression alterations in C57BL/6J and ICAM-I-deficient mice. *Am J Physiol Endocrinol Metabol* 282: E703-E713, 2002.

Guiherme A, Virbasius JV, Puri V, Czech MP. Adipocyte dysfunctions linking obesity to insulin resistance and type 2 diabetes. *Nat Rev Mol Cell Biol* 9: 367-377, 2008.

Hess DT, Matsumoto A, Kim SO, Marshall HE, Stamler JS. Protein S-nitrosylation: purview and parameters. *Nat Rev Mol Cell Bio* 6: 150-155, 2005.

Huang PL. eNOS, metabolic syndrome and cardiovascular disease. *Trends Endocrinol Metab* 20: 295-302, 2009.

Jiang H, Torregrossa AC, Potts A, Pierini D, Aranke M, Garg HK, Bryan NS. Dietary nitrite improves insulin signaling through GLUT4 translocation. *Free Rad Biol Med* 67: 51-57, 2014.

Kim S, Sohn I, Ahn JI, Lee KH, Lee YS, Lee YS. Hepatic gene expression profiles in a long-term high-fat diet-induced obesity mouse model. *Gene* 340: 99-109, 2004.

Khoo NKH, Mo L, Zharikov S, Kamga C, Quesnelle K, Golin-Bisello F, Li L, Wang Y, Shiva Sruti. Nitrite augments glucose uptake in adipocytes through the protein kinase A-dependent stimulation of mitochondrial fusion. *Free Radic Biol Med* 70: 45-53, 2014.

Knobeloch L, Salna B, Hogan A, Postle J, Anderson H. Blue babies and nitrate-contaminated well water. *Environ Health Persp* 108: 657-678, 2000.

Kobayashi J, Ohtake K, Uchida H. NO-rich diet for lifestyle-related diseases. *Nutrients* 7: 4911-4937, 2015.

Konopelska S, Kienitz T, Quinkler M. Downregulation of hepatic glucose-6-phosphatase-α in patients with hepatic steatosis. *Obesity* 19: 2322-2326, 20211.

Knopp RH, Zhu X, Bonet B. Effects of estrogens on lipoprotein metabolism and cardiovascular disease in women. *Atherosclerosis* 110: S83–S91, 1994.

Larsen FJ, Schiffer TA, Borniquel S ,Sahlin K, Ekblom B, Lundberg JO, Weitzberg E. Dietary inorganic nitrate improves mitochondrial efficiency in humans. *Cell Metab* 13: 149-159, 2011.

Lim JH, Gerhart-Hines Z, Dominy JE, Lee Y, Kim S, Tabata M, Xiang YK, Puigserver P. Oleic acid stimulates complete oxidation of fatty acids through protein kinase A-dependent activation of SIRT1-PGC1α complex. *J Biol Chem* 288:7117-7126, 2013.

Lin S, Thomas TC, Storlien LH, Huang XF. Development of high fat diet-induced obesity and leptin resistance in C57BL/6J mice. *Int J Obes Relat Metab Disord* 24: 639-646, 2000.

Liu M, Wu K, Mao X, Wu Y, Ouyang J. Astragalus polysaccharide improves insulin sensitivity in KKA^{y} mice: regulation of PKB/GLUT4 signaling in skeletal muscle. *J Ethnopharmacol* 127:32-37, 2010.

Ludgero-Correia A, Aguila MB, Mandarim-de-Lacerda CA, Faria TS. Effects of high-fat diet on plasma lipids, adiposity, and inflammatory markers in ovariectomized C57BL/6 mice. *Nutrition* 28: 316-323, 2012.

Majmudar NG, Robson SC, Ford GA. Effects of the menopause, gender, and estrogen replacement therapy on vascular nitric oxide activity. *J Clin Endocr Metab* 85: 1577-1583, 2000.

Monti LD, Barlassina C, Citterio L, Galluccio E, Berzuini C, Setola E, Valsecchi G, Lucotti P, Pozza G, Bernardinelli L, Casari G, Piatti P. Endothelial nitric oxide synthase polymorphisms are associated with type 2 diabetes and the insulin resistance syndrome. *Diabetes* 52: 1270-1275, 2003.

Murano I, Barbatelli G, Parisani V, Latini C, Muzzonigro G, Castellucci M, Cinti S. Dead adipocytes, detected as crown-like structures, are prevalent in visceral fat depots of genetically obese mice. *J Lipid Res* 49: 1562-1568, 2008.

Murase T, Mizuno T, Omachi T, Onizawa K, Komine Y, Kondo H, Hase T, Tokimitsu I. Dietary diacylglycerol suppresses high fat and high sucrose diet-induced body fat accumulation in C57BL/6J mice. *J Lipid Res* 42: 372-378, 2001.

Nystrom T, Ortsater H, Huang Z, Zhang F, Larsen FJ, Weitzberg E, Lundberg JO, Sjoholm A. Inorganic nitrite stimulates pancreatic islet blood flow and insulin secretion. *Free Radic Biol Med* 53: 1017-1023, 2012.

Ohtake K, Ishiyama Y, Uchida H, Muraki E, Kobayashi J. Dietary nitrite inhibits early glomerular injury in streptozotocin-induced diabetic nephropathy in rats. *Nitric Oxide* 17:75-81, 2007.

Ohtake K, Koga M, Uchida H, Sonoda K, Ito J, Uchida M, Natsume H, Kobayashi J. Oral nitrite ameliorates dextran sulfate sodium-induced acute experimental colitis in mice. *Nitric Oxide* 23: 65-73, 2010.

Okuno A, Tamemoto H, Tobe K, Ueki K, Mori Y, Iwamoto K, Umesono K, Akanuma Y, Fujiwara T, Horikoshi H, Yazaki Y, Kadowaki T. Troglitazone increases the number of small adipocytes without the change of white adipose tissue mass in obese Zucker rats. *J Clin Invest* 101: 1354-1361, 1998.

Reeves PG, Nielsen FH, Fahey GC Jr. AIN-93 purified diets for laboratory rodents: final report of the American Institute of Nutrition ad hoc writing committee on the reformulation of the AIN-76A rodent diet. *J Nutr* 123:1939-1951, 1993.

Rizzo NO, Maloney E , PhamM, Luttrell I, Wessells H, Tateya S, Daum G, Handa P , Schwartz MW, Kim F. Reduced NO-cGMP Signaling Contributes to Vascular Inflammation and Insulin Resistance Induced by High-Fat Feeding. *Arterioscler Thromb Vasc Biol* 30: 758-765, 2010.

Shoelson SE, Lee J, Goldfine AB. Inflammation and insulin resistance. *J Clin Invest* 116: 1793-1801, 2006.

Stokes KY, Dugas TR, Tang Y, Garg H, Guidry E, Bryan NS. Dietary nitrite prevents hypercholesterolemic microvascular inflammation and reverses endothelial dysfunction. *Am J Physiol Heart Circ Physiol* 296: H1281-H1288, 2009.

Tachibe M, Kato R, Kishida T, Ebihara K. Hydroxypropylated tapioca starch retards the development of insulin resistance in KKAy mice, a Type 2 diabetes model, fed a high-fat diet. *J Food Sci* 74: H232-H236.

Wang H, Wang AX, Aylor K, Barrett EJ. Nitric oxide directly promotes vascular endothelial insulin transport. *Diabetes* 62: 4030-4042, 2013.

Wang Y, Shoemaker R, Thatcher SE, Batifoulier-Yiannikouris F, English VL, Cassis LA. Administration of 17β-estradiol to ovariectomized obese female mice reverses obesity-hypertension through an ACE2-dependent mechanism. *Am J Physiol Endocrinol Metab* 308: E1066-E1075, 2015.

Yamamoto T, Shimano H, Nakagawa Y, Ide T, Yahagi N, Matsuzaka T, Nakakuki M, Takahashi A, Suzuki H, Sone H, Toyoshima H. Sato R, Yamada N. SREBP-1interacts with hepatocyte nuclear factor-4 alpha and interferes with PGC-1 recruitment to suppress hepatic gluconeogenic genes. *J Biol Chem* 279: 12027-12035, 2004.

Yuan M, Konstantopoulos N, Lee J, Hansen L, Li ZW, Karin M, Shoelson SE. Reversal of obesity- and diet-induced insulin resistance with salicylates or targeted disruption of Ikkβ. *Science* 293: 1673-1677, 2001.

LEGENDS

Figure 1

Effect of dietary fat and nitrite on body mass

(A) The effects of dietary high fat and nitrite on the uterine mass of mice treated with or without OVX. Significant difference between sham (NF and HF) and OVX+HF groups (0, 50, and 150 mg nitrite) from 1 week to 17 weeks, $p<0.05$. Sham+NF vs. sham+HF, significant from 4 week to 17 weeks, $p<0.05$. No significant differences among OVX+HF groups.

(B) Time course of body weight change of sham or OVX mice treated with or without dietary high fat and nitrite. $^{a}p<0.05$ vs. sham+NF, $^{b}p<0.05$ vs. sham+HF, Mean±SE.

NF: normal fat, HF: high fat, OVX: ovariectomized, N50: nitrite 50mg/L, N150: nitrite 150mg/L

○: sham+NF, △: sham+HF, □: OVX+HF, ●: OVX+HF+N50, ▲: OVX+HF+N150. The results are shown as the means ± SE (n=8).

Figure 2

Effect of HF diet and dietary nitrite on morphometry of visceral adipocytes

(A) The ratio of ovarian fat mass to whole body mass (g/kg body weight) in the 5 groups.

(B) Light micrographs showing adipocytes in the visceral fat pad (×200). Arrow indicates the presence of inflammatory infiltrate in OVX+HF group (crown-like structure).

(C) The size of ovarian adipocyte (μm^2/cell) in the 5 groups.

NF: normal fat, HF: high fat, OVX: ovariectomized, N50: nitrite 50 mg/L, N150: nitrite 150 mg/L

$^{a}p<0.05$ vs. sham+NF, $^{b}p<0.05$ vs. sham+HF, $^{c}p<0.05$ vs. OVX+HF. The results are shown as the means ± SE (n=8).

Figure 3

Transcriptional levels of the biomarkers in ovarian adipose tissue

(A) The mRNA levels of TNF-α, IL-6, and MCP-1 in the 5 groups.

(B) The mRNA levels of adiponectin, β_3-adrenergic receptor, UCP-1, PPAR-γ, C/EBP-α in the 5 groups. The mRNA levels are standardized by GAPDH mRNA

IL-6: interleukin-6, TNF-α: tumor necrosis factor-α, MCP-1: monocyte chemoattractant protein-1, GAPDH: glyceraldehyde-3-phosphate dehydrogenase, UCP-1: uncoupling protein-1, PPAR-γ: peroxisome proliferator-activated receptor-γ, C/EBP-α: CCAAT/enhancer-binding protein-α.

NF: normal fat, HF: high fat, OVX: ovariectomized, N50: nitrite 50mg/L, N150: nitrite 150mg/L

$^{a}p<0.05$ vs. sham+NF, $^{b}p<0.05$ vs. sham+HF, $^{c}p<0.05$ vs. OVX+HF. The results are shown as the means ± SE (n=8).

Figure 4
Effect of dietary nitrite on OVX and HF diet-induced fatty liver.
(A) Representative histomorphology of liver in the 5 groups.
(B) The ratio of the total fat vacuole area in liver section (×200).
NF: normal fat, HF: high fat, OVX: ovariectomized, N50: nitrite 50 mg/L, N150: nitrite 150 mg/L.

Figure 5 *Transcriptional levels of the metabolic factors in liver.*
The hepatic mRNA levels of SREBP-1c, ACC, ACO, MCAD, G6Pase, and PAPCK.
SREBP-1c: sterol regulatory element binding protein-1c, ACC: acetyl-CoA carboxylase, ACO: acyl-CoA oxidase, MCAD: middle-chain acyl-CoA dehydrogenase, G6Pase: glucose-6-phosphatase, PEPCK: phosphoenolpyruvate carboxykinase, NF: normal fat, HF: high fat, OVX: ovariectomized, N50: nitrite 50 mg/L, N150: nitrite 150 mg/L
$^{a}p<0.05$ vs. sham+NF, $^{b}p<0.05$ vs. sham+HF, $^{c}p<0.05$ vs. OVX+HF. The results are shown as the means ± SE (n=8).

Figure 6
Effect of dietary nitrite on glucose metabolism and insulin sensitivity
Fasting plasma levels of glucose (A), insulin (B) and HOMA-IR(C) in the 5 groups.
HOMA-IR : the homeostasis model assessment as an index of insulin resistance.
NF: normal fat, HF: high fat, OVX: ovariectomized, N50: nitrite 50 mg/L, N150: nitrite 150 mg/L
$^{a}p<0.05$ vs. sham+NF, $^{b}p<0.05$ vs. sham+HF, $^{c}p<0.05$ vs. OVX+HF. The results are shown as the means ± SE (n=8).

Figure 7
Plasma levels of nitrate/nitrite
NF: normal fat, HF: high fat, OVX: ovariectomized, N50: nitrite 50 mg/L, N150: nitrite 150 mg/L
$^{a}p<0.05$ vs. sham+NF. The results are shown as the means ± SE (n=8).

Figure 1

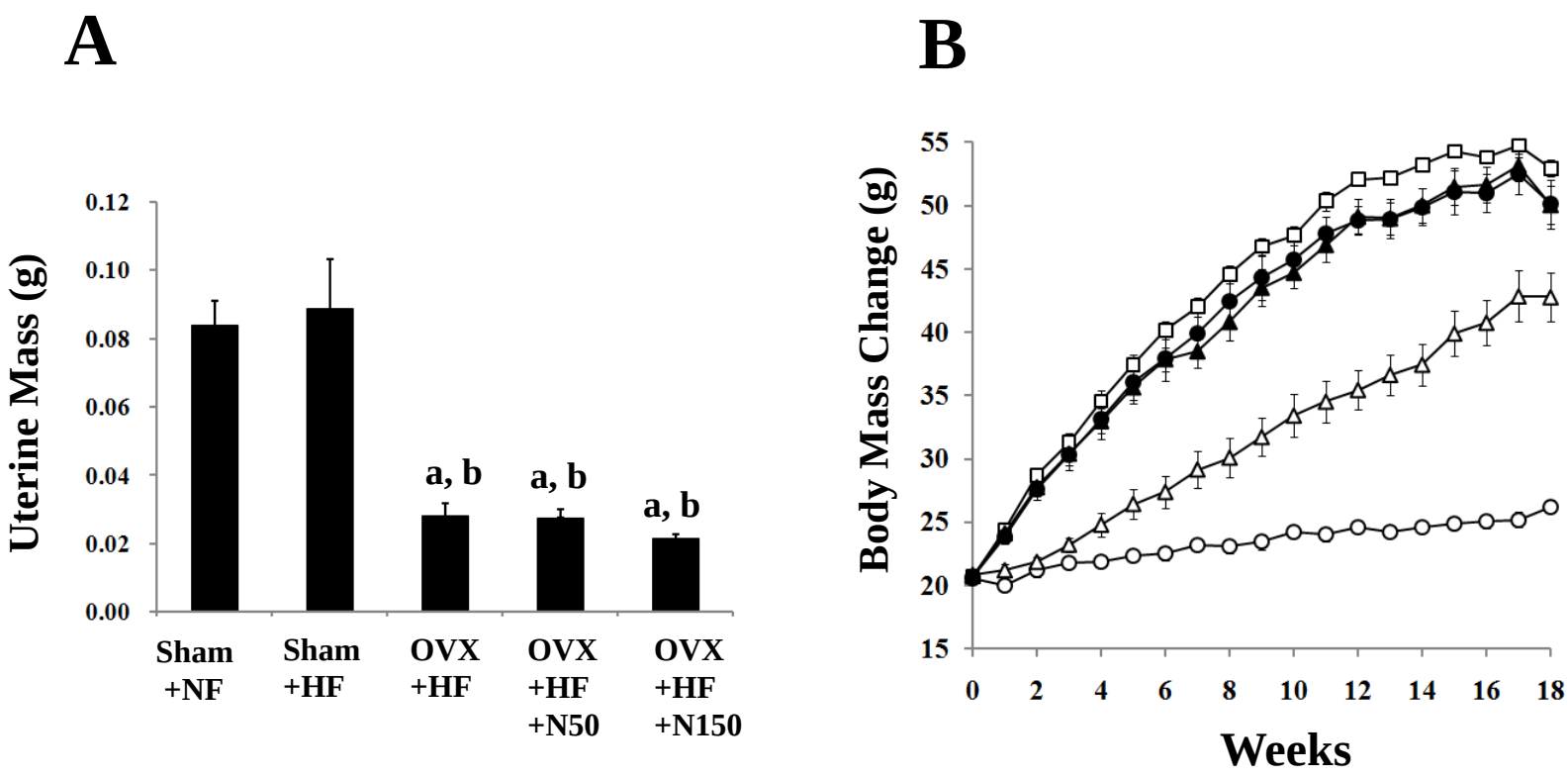
A
Uterine Mass (g)
0.12
0.10
0.08
0.06
0.04
0.02
0.00
a, b
a, b
a, b
Sham +NF
Sham +HF
OVX +HF
OVX +HF +N50
OVX +HF +N150
B
Body Mass Change (g)
55
50
45
40
35
30
25
20
15
0
2
4
6
8
10
12
14
16
18
Weeks

Figure 2

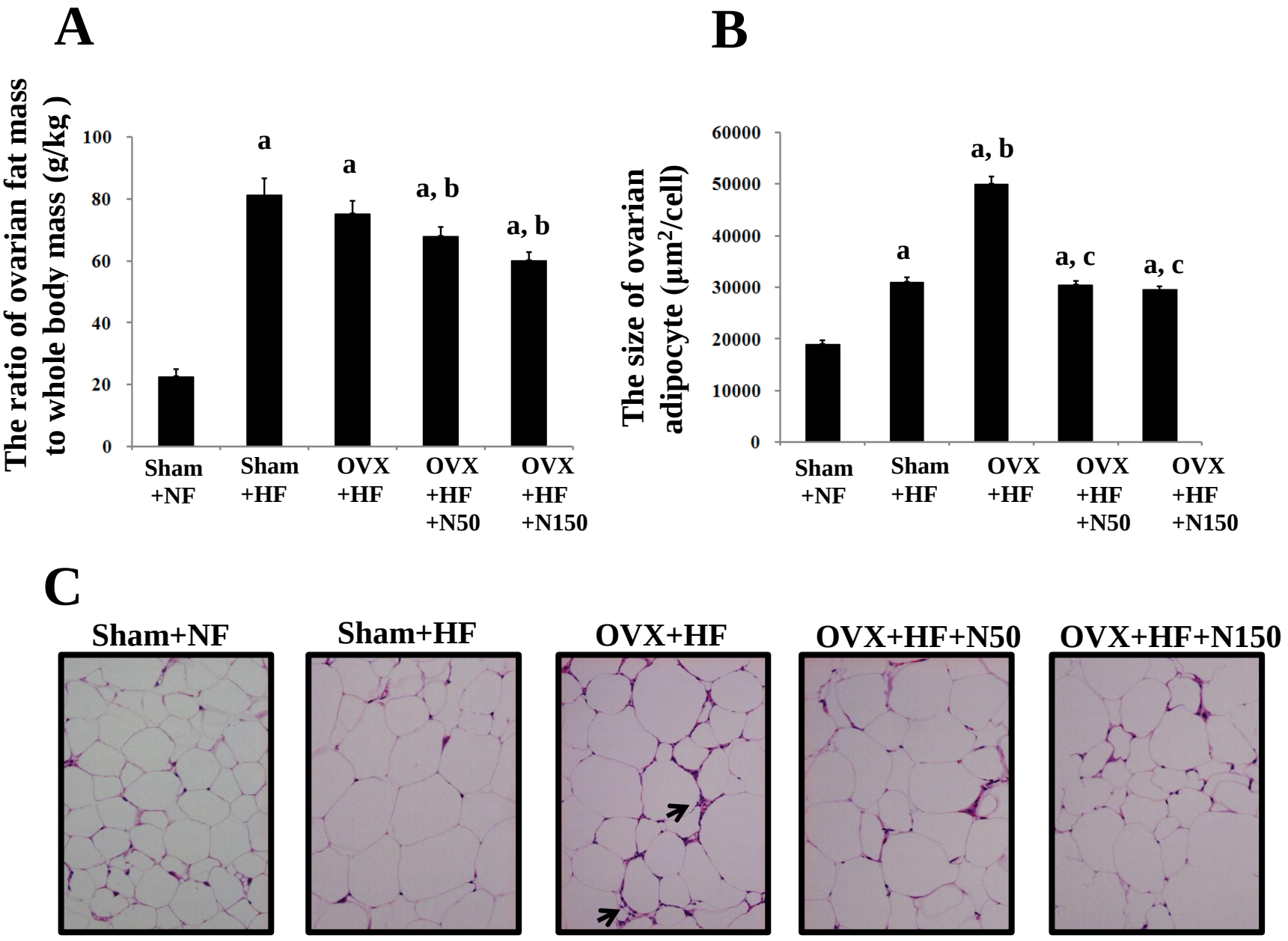
A
The ratio of ovarian fat mass to whole body mass (g/kg)
100
80
60
40
20
0
a
a
a, b
a, b
Sham +NF
Sham +HF
OVX +HF
OVX +HF +N50
OVX +HF +N150
B
The size of ovarian adipocyte (μm²/cell)
60000
50000
40000
30000
20000
10000
0
a
a, b
a, c
a, c
Sham +NF
Sham +HF
OVX +HF
OVX +HF +N50
OVX +HF +N150
C
Sham+NF
Sham+HF
OVX+HF
OVX+HF+N50
OVX+HF+N150

Figure 3

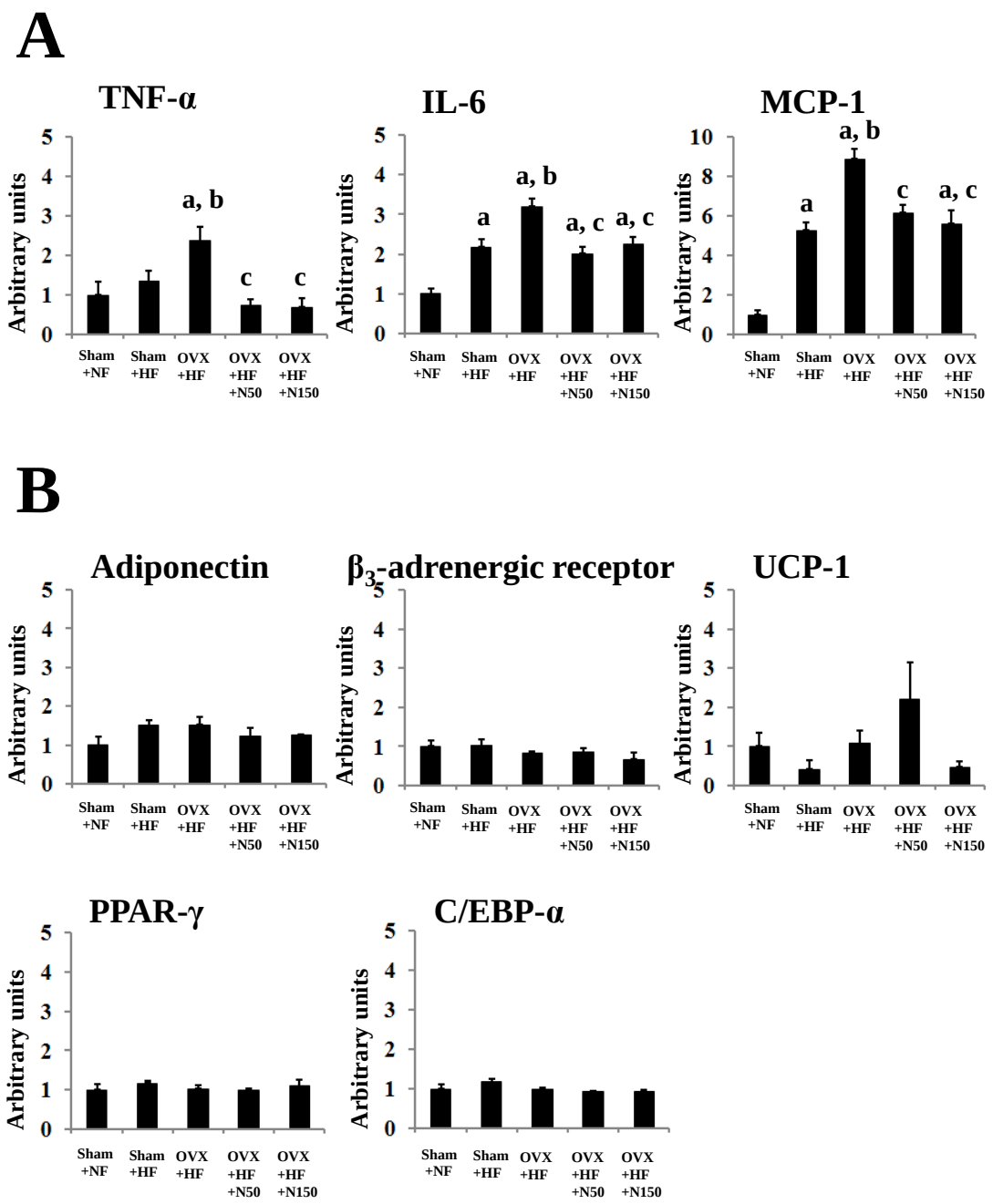
A
TNF-α
IL-6
MCP-1
Arbitrary units
a, b
c
c
a
a, b
a, c
a, c
a
a, b
c
a, c
Sham +NF
Sham +HF
OVX +HF
OVX +HF +N50
OVX +HF +N150
B
Adiponectin
β3-adrenergic receptor
UCP-1
PPAR-γ
C/EBP-α

Figure 4

A

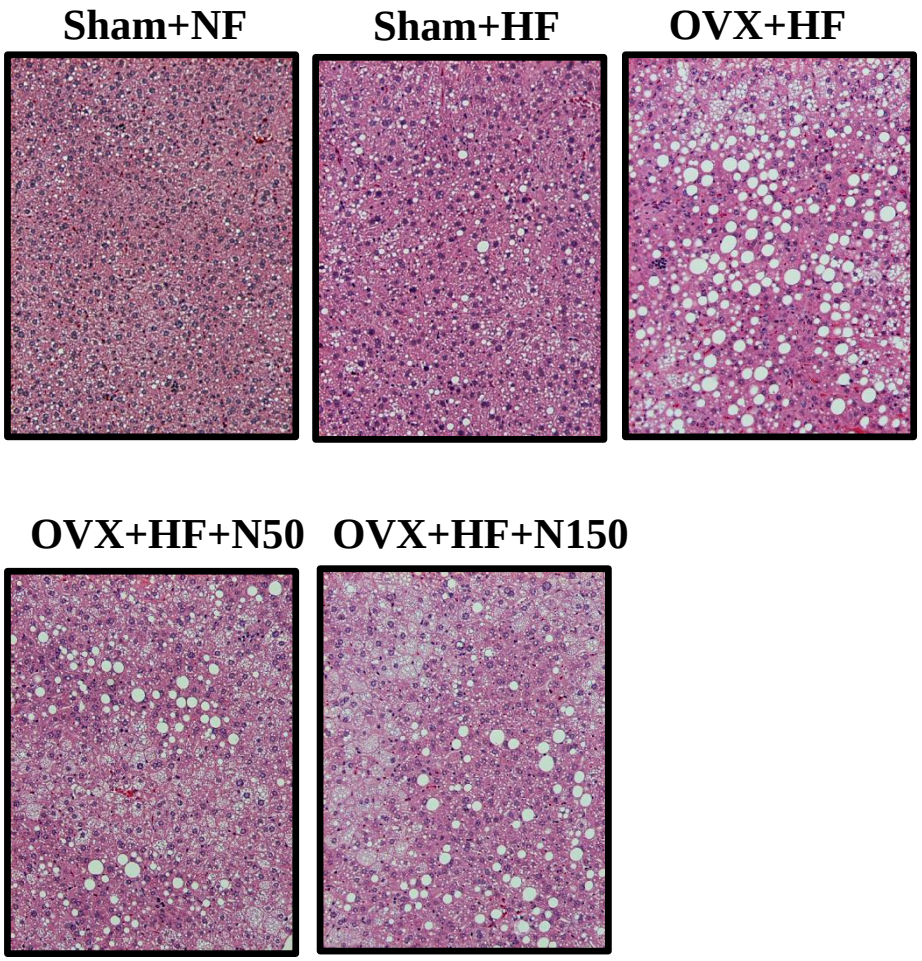
Sham+NF
Sham+HF
OVX+HF
OVX+HF+N50
OVX+HF+N150

B

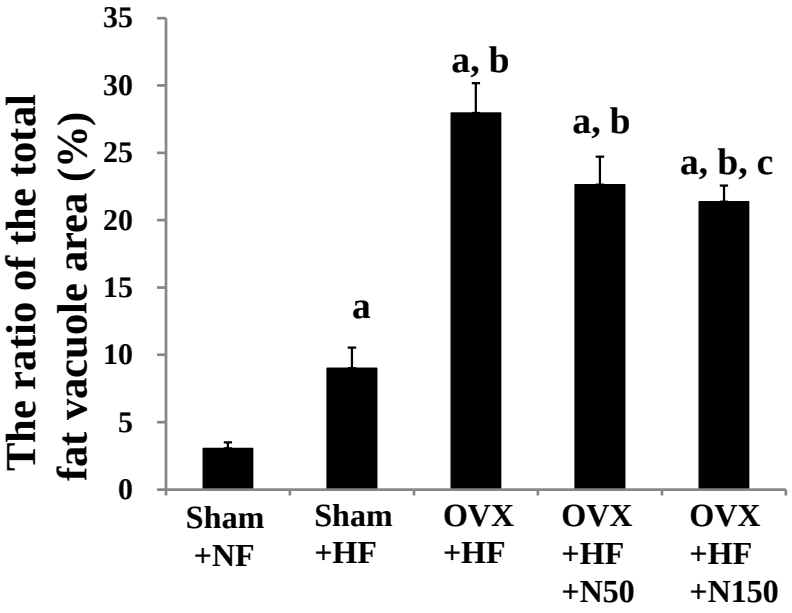
The ratio of the total fat vacuole area (%)
35
30
25
20
15
10
5
0
a
a, b
a, b
a, b, c
Sham +NF
Sham +HF
OVX +HF
OVX +HF +N50
OVX +HF +N150

Figure 5

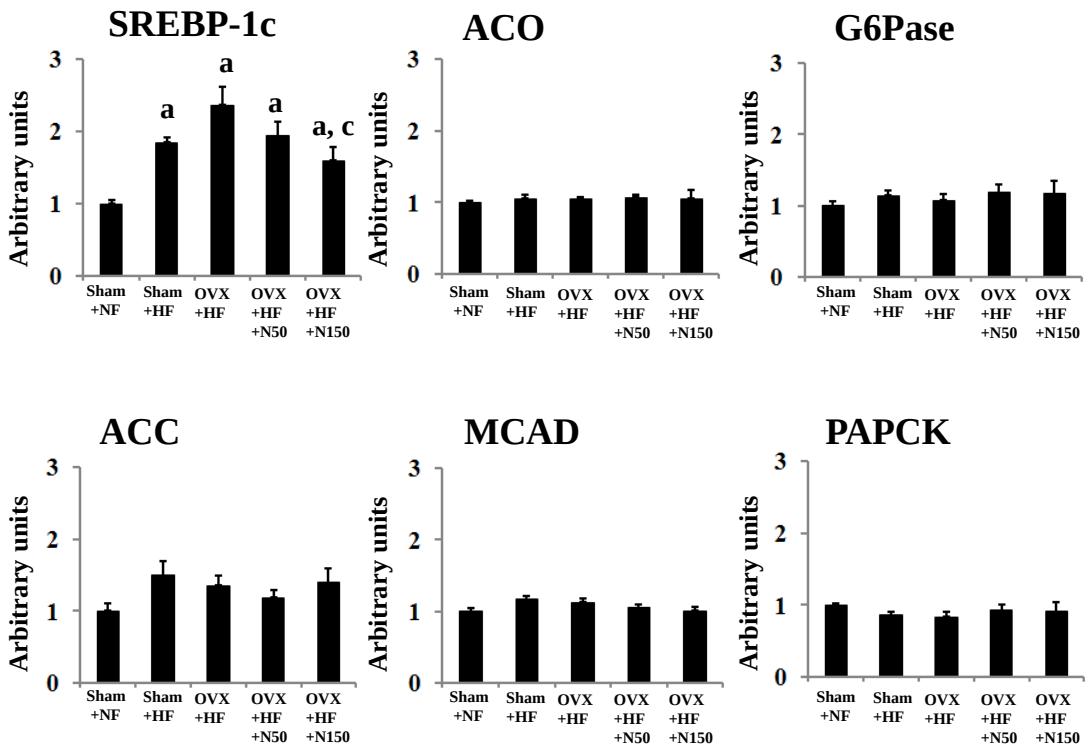
SREBP-1c
ACO
G6Pase
ACC
MCAD
PAPCK
Arbitrary units
0
1
2
3
a
a
a
a, c
Sham +NF
Sham +HF
OVX +HF
OVX +HF +N50
OVX +HF +N150

Figure 6

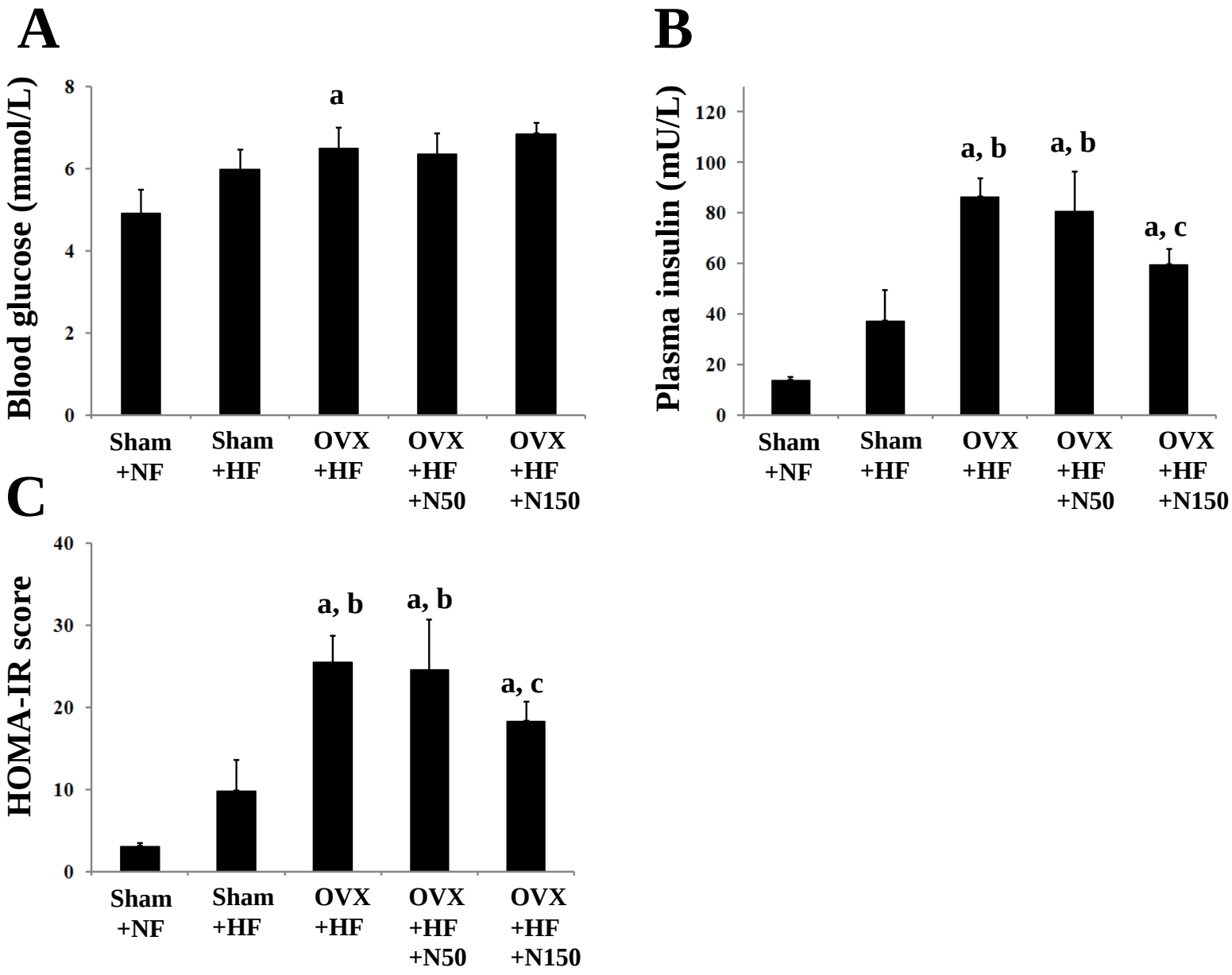
A
Blood glucose (mmol/L)
8
6
4
2
0
a
Sham +NF
Sham +HF
OVX +HF
OVX +HF +N50
OVX +HF +N150
B
Plasma insulin (mU/L)
120
100
80
60
40
20
0
a, b
a, b
a, c
Sham +NF
Sham +HF
OVX +HF
OVX +HF +N50
OVX +HF +N150
C
HOMA-IR score
40
30
20
10
0
a, b
a, b
a, c
Sham +NF
Sham +HF
OVX +HF
OVX +HF +N50
OVX +HF +N150

Figure 7

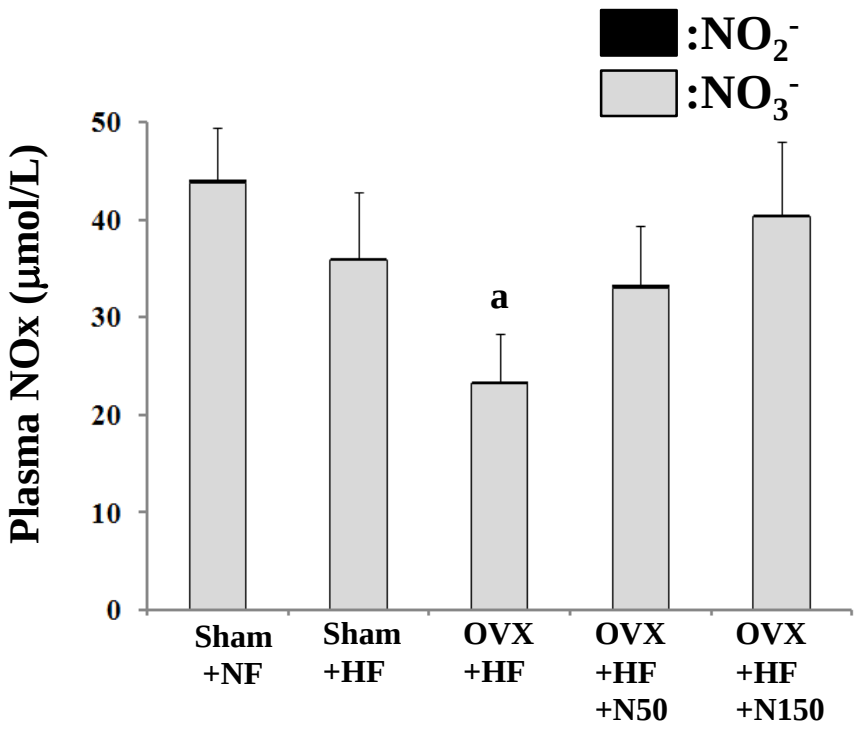
:NO2-
:NO3-
Plasma NOx (µmol/L)
50
40
30
20
10
0
a
Sham +NF
Sham +HF
OVX +HF
OVX +HF +N50
OVX +HF +N150